

Special  
Collection

# Recent Trends in Chiroptical Spectroscopy: Theory and Applications of Vibrational Circular Dichroism and Raman Optical Activity

Monika Krupová,<sup>[a, b]</sup> Jiří Kessler,<sup>[a]</sup> and Petr Bouř<sup>\*[a]</sup>



Chiroptical spectroscopy exploring the interaction of matter with polarized light provides many tools for molecular structure and interaction studies. Here, some recent discoveries are reviewed, primarily in the field of vibrational optical activity. Technological advances result in the development of more sensitive vibrational circular dichroism (VCD), Raman optical activity (ROA) or circular polarized luminescence (CPL) spectrometers. Significant contributions to the field also come from the light scattering and electronic structure theories, and their

implementation in computer systems. Finally, new chiroptical phenomena have been observed, such as enhanced circular dichroism of biopolymers (protein fibrils, nucleic acids), plasmonic and resonance chirality-transfer ROA experiments. Some of them are not yet understood or attributed to instrumental artifacts so far. Nevertheless, these unknown territories also indicate the vast potential of the chiroptical spectroscopy, and their investigation is even more challenging.

## Introduction

Chiroptical spectroscopy has many faces. One can mention the almost metaphysical question why the life on Earth is based on chiral (possessing the left- and right-hand symmetry) molecules, how the symmetry was broken, and if other life forms were possible.<sup>[1]</sup> This has clear implication for space exploration research.<sup>[2]</sup> Deeply in fundamental physics, a fascinating fact appeared in 1950s, when a weak preference of our universe for particular enantiomeric forms was discovered.<sup>[3]</sup>

In a more applied vein, which we are more competent to comment on, the spectroscopy is being constantly developed by many researchers to tools useful, for example, in chemistry, biology and medicine. Even though we would like to focus on the present state, to understand the varieties of the experiment one has to realize that the foundations were laid already by people like Luis Pasteur,<sup>[4]</sup> who connected polarization of light with molecular geometry properties, and Michael Faraday,<sup>[5]</sup> who noticed that similar or additional effect can be achieved by placing the sample in the magnetic field.

As of now, several spectroscopic techniques using the polarized light exist, and several phenomena concerning interaction of the light with matter are known, although some of them are rarer and some are used more regularly (Table 1). Of course, in the table, the list is quite simplified. For example, some electronic transitions may lie in the “vibrational” region and be measurable with the infrared optics, natural and magnetic optical activity can be measured at the same time, etc. Outside the scope of this review, but worthy to mention, are detection techniques allowing to combine optical activity with time resolution of very fast processes.<sup>[6,7]</sup>

We focus on the vibrational optical activity and associated experiments, which are perhaps less known than the electronic spectroscopy, in particular the omnipresent electronic circular dichroism, but which have been very dynamically evolving in the past years. Below, basic terms and quantities concerning absorption, emission and scattering of polarized light are

introduced, and selected recent discoveries concerning the “classical” or newer chiroptical spectroscopies are discussed, perhaps indicating future directions of the field.

## Basic Terms and Quantities

Before going to particular examples, it may be useful to mention the physical basis, such as that the simplest form of polarized light is the plane wave. Alternatively, one can go to more general description in quantum electrodynamics,<sup>[17]</sup> not needed, however, for the most common experiments. Propagating the wave along the z-direction, the light can be *linearly polarized* so that the vector of electric intensity **E** oscillates, for example, along the x and y-directions,

**Table 1.** Broad classes of chiroptical methods.

	Electronic Transitions	Vibrational Transitions
<b>Natural Chirality:</b>		
Optical rotatory dispersion (ORD)	standard method, now often replaced by ECD	not much used, may become more common in the future
Circular dichroism (CD)	electronic CD (ECD), a standard method, commercialized	vibrational CD (VCD), observed in 1970s, <sup>[8]</sup> commercial spectrometer <sup>[9]</sup> from 1997
Circularly polarized luminescence (CPL)	starting to be commercially available	unknown
Raman optical activity (ROA)	unexplored	observed in 1973, <sup>[10]</sup> commercial apparatus <sup>[11]</sup> available from ~2005
<b>Magnetic Analogues:</b>		
Magnetic ORD	the Faraday effect	unused
Magnetic CD, MCD	MCD, fairly standard technique	MVCD, observed in 1984, <sup>[12]</sup> explained in 2018, <sup>[13]</sup> rather rare
Magnetic CPL	fairly available, rather rare	unknown
Magnetic ROA	unexplored	possible in resonance, <sup>[14]</sup> even for gases <sup>[15,16]</sup>

[a] M. Krupová, Dr. J. Kessler, Prof. P. Bouř  
Institute of Organic Chemistry and Biochemistry Academy of Sciences  
Flemingovo náměstí 2, 16610 Prague (Czech Republic)  
E-mail: bour@uochb.cas.cz

[b] M. Krupová  
Faculty of Mathematics and Physics  
Charles University  
Ke Karlovu 3, 12116 Prague 2 (Czech Republic)



This article is part of a Special Collection on “Chemistry in the Czech Republic”.

$$E^x = \begin{pmatrix} 1 \\ 0 \\ 0 \end{pmatrix} E_0^x \cos(\omega t - kz)$$

$$E^y = \begin{pmatrix} 0 \\ 1 \\ 0 \end{pmatrix} E_0^y \cos(\omega t - kz + \varphi)$$
(1)

where  $\omega$  is the angular frequency,  $t$  is time,  $k$  is the  $z$ -component of the wave vector,  $\varphi$  is a phase delay,  $E_0^x$  and  $E_0^y$  are constants. By combination of these two  $x$  and  $y$  components, different *elliptical polarizations* arise. Special cases are left and right *circular polarizations*, when the components have the same amplitudes, but one is “delayed” by  $\varphi = \pi/2$ , providing right and left-circularly polarized lights with electric intensities

$$E^R = \begin{pmatrix} \cos(\omega t - kz) \\ \sin(\omega t - kz) \\ 0 \end{pmatrix} E_0$$

$$E^L = \begin{pmatrix} \cos(\omega t - kz) \\ -\sin(\omega t - kz) \\ 0 \end{pmatrix} E_0$$
(2)

The tips of the  $E^R$  and  $E^L$  vectors follow a helix in space, which is tremendously important for chemistry, because such light may selectively interact with chiral molecules possessing the “screw” or “hand” symmetry. We also see that the circular polarization can be made from the linear polarization, and vice versa, which is fairly easy to do with common optical elements. This enhances making and detection of the polarization, keeping the instrumentation relatively “cheap” and versatile,

obviously in comparison to other more complicated techniques, such as x-ray crystallography, NMR or transmission electron cryomicroscopy.

Molecules “see” the light through the interaction potential  $V$ .<sup>[14]</sup> In the simplest form, we may consider

$$V = \boldsymbol{\mu} \cdot \mathbf{E} - \boldsymbol{\Theta} \cdot \nabla E - \mathbf{m} \cdot \mathbf{B},$$
(3)

where  $\boldsymbol{\mu}$  is the electric dipole,  $\boldsymbol{\Theta}$  is the electric quadrupole,  $\mathbf{m}$  is the magnetic dipole, and  $\mathbf{B}$  is the magnetic field. One “weak point” of chiroptical spectroscopy is that the last two terms containing  $\boldsymbol{\Theta}$  and  $\mathbf{m}$ , sensitive to the chiral symmetry, are usually much smaller than the first insensitive one. As a rule of thumb, ratio of the chiral and achiral parts in a spectrum is approximately proportional to  $a/\lambda$ , where  $a$  is dimension of a molecule, and  $\lambda$  is wavelength of the light.

The “ $a/\lambda$ ” obstacle can be well-illustrated on circular dichroism (CD), which measures difference of absorption indices of left- and right circularly polarized light,

$$\Delta\varepsilon(CD) = \varepsilon_L - \varepsilon_R,$$
(4)

or circular polarized luminescence (CPL), detecting corresponding intensity differences,

$$\Delta I(CPL) = I_L - I_R$$
(5)

For electronic transitions typically associated with big energies and short wavelengths ( $\lambda \sim 200\text{--}1000$  nm) the “dissymmetry” factor

$$g = 2(\varepsilon_L - \varepsilon_R)/(\varepsilon_L + \varepsilon_R).$$
(6)

relating  $\Delta\varepsilon$  (electronic CD, ECD) to total absorption is about  $10^{-3}$  for common molecules.<sup>[18]</sup> For VCD, however, about ten-times longer wavelengths are used, and  $g$  is often smaller than  $10^{-4}$ , requiring more elaborate detection.<sup>[19]</sup> Even worse situa-



Monika Krupová obtained her bachelor's degree in biochemistry and master's degree in biophysical chemistry at the Charles University, Prague. Currently, she is a PhD student in physics at the Charles University, Faculty of Mathematics and Physics, and at the Institute of Organic Chemistry and Biochemistry of the Czech Academy of Sciences. Her research interests focus on the application of chiroptical spectroscopy methods to biological systems.



Jiří Kessler is currently a researcher in the Molecular Spectroscopy group at the Institute of Organic Chemistry and Biochemistry. He obtained his PhD degree at the Charles University in Prague, under the guidance of Prof. P. Bouř in 2017, in the field of biomolecular spectroscopy. His research interests include computational chemistry and spectroscopy of vibrational optical activity.



Petr Bouř obtained his master's degree in physics at the Charles University, Prague, and the CSc. degree (PhD equivalent, 1993) in organic chemistry at the Czechoslovak Academy of Sciences, Prague, in a joint program with the University of Illinois at Chicago. Since 2007 he has been the leader of the Molecular Spectroscopy group in the Institute of Organic Chemistry and Biochemistry and in 2013, he became professor in Analytical Chemistry at the University of Chemistry and Technology, Prague. His research interests comprise the development of molecular dynamics and quantum chemical computational procedures for spectroscopy, as well as experimental and theoretical aspects of vibrational optical activity. He published about 200 research articles and 4 book chapters.

tion is expected for microwave (rotational) CD, with expected  $g \sim 10^{-5}$ – $10^{-6}$ , which is one of the reasons why rotational CD has been explored only theoretically so far.<sup>[20]</sup>

Vibrational Raman optical activity (ROA) is defined in an opposite way to CPL ("right minus left"), as

$$\Delta I (\text{ROA}) = I_R - I_L \quad (7)$$

and in analogy to the  $g$ -factor, circular intensity difference is usually used, defined as

$$CID = (I_R - I_L)/(I_R + I_L). \quad (8)$$

Unlike CD or CPL, Raman scattering is a two-photon process. However, it is driven by the same interaction potential and we can thus deduce that typical value of  $CID$  will be  $10^{-4}$ , similar to the case of VCD.

The ROA measurement is facilitated by using the visible light, but the underlying Raman signal is already much weaker ( $\sim 10^6$  times!) than the input beam. VCD theory and experiment are simpler, measurement of the unpolarized absorption is relatively easy, but processing and detection of the infrared light are difficult, which results to about the same signal to noise (S/N) ratio for both techniques.

The weak signal in VCD and ROA typically requires concentrated samples and long accumulation times, prohibitive for many applications. Therefore, several enhancement mechanisms, discovered relatively recently both for VCD and ROA, acquired widespread attention.

## Vibrational Circular Dichroism

### Molecular Vibrational Circular Dichroism

The VCD technique is probably the most common vibrational optical activity spectroscopy today, becoming a standard in absolute configuration determination and molecular conformational studies. Also from the point of theory, the effect seems to be well understood, in spite of initial problems related to the description of VCD within the Born-Oppenheimer approximation.<sup>[21]</sup> The first experiments<sup>[8]</sup> were followed by many applications, such as those involving proteins and peptides,<sup>[22–29]</sup> or nucleic acids.<sup>[30–36]</sup>

The experimental advances of VCD spectroscopy have been encouraged by the possibility to calculate the spectra, in particular using the density functional theory (DFT).<sup>[37]</sup> Similarly as for CPL or electronic CD, VCD band area is proportional to the rotational strengths ( $R$ ), whereas for plain absorption/luminescence it is proportional to the dipole strength ( $D$ ) for each transition  $i \rightarrow f$ .<sup>[38]</sup>

$$\begin{aligned} R &= \text{Im} \mu_{if} \cdot m_{fi} \\ D &= \mu_{if} \cdot \mu_{fi} \end{aligned} \quad (9)$$

where  $\mu_{if}/m_{fi}$  are the transition electric/magnetic dipole moments.

Relations (9) are valid for isotropic samples (liquids, solutions). For some cases discussed below (condensation, crystals) other terms may contribute to VCD and IR intensities, which then become orientation-dependent.<sup>[14]</sup>

For vibrational transitions and the harmonic approximation, the moments can be further elaborated to

$$\begin{aligned} m_{if,\alpha} &= \sqrt{2\hbar^3\omega_i} \sum_{\lambda,\beta} A_{\alpha,\lambda\beta} S_{i,\lambda\beta}, \\ \mu_{if,\alpha} &= \sqrt{\frac{\hbar}{2\omega_i}} \sum_{\lambda,\beta} P_{\alpha,\lambda\beta} S_{i,\lambda\beta}, \end{aligned} \quad (10)$$

where  $\hbar$  is the reduced Planck constant,  $\omega_i$  is vibrational frequency,  $S$  is the Cartesian-normal mode transformation matrix, and  $A$  and  $P$  are atomic axial and polar tensors, respectively. Different definitions of  $A$  and  $P$  exist in literature; in any case all quantities in eqs. (9) and (10) are available from many computer programs. VCD can thus be today simulated using accurate methods of quantum chemistry.

For bigger molecules, however, interpretation of VCD based on the simulations may be problematic, because of an excessive computational time. In this case, empirical models can be used, but their accuracy is limited.<sup>[39,40]</sup> As a better alternative, we proposed the Cartesian coordinate-based tensor transfer ("CCT"), where the vibrational parameters - force field, magnetic and electric dipole derivatives (tensors  $A$  and  $P$ ) - are calculated for smaller fragments and transferred back on the molecule of interest.<sup>[41]</sup> This allowed for relatively precise<sup>[42,43]</sup> VCD simulations on sizable polypeptides and proteins<sup>[44–46]</sup> or nucleic acids.<sup>[47,48]</sup> Lately, technologically more advanced molecules-in-molecules (MIM) method has been developed and applied on several examples, although systems studied by it were still smaller than allowed by CCT.<sup>[49–51]</sup>

In the computations, a realistic model of the solvent is always beneficial. This is particularly true for VCD, because the biggest signal usually comes from polar groups, very much interacting with the environment.<sup>[52–54]</sup> The solvent can be included as a polarizable continuum model (PCM)<sup>[55,56]</sup> or by "explicit" solvation, where studied molecule is surrounded by a few solvent molecules. The latter case is sometimes referred to as a combination of quantum mechanics and molecular mechanics methods, QM/MM, or multi-scale approach.<sup>[57–60]</sup> The "explicit" clusters can also be surrounded by a PCM continuum, to account for longer-range solvent effects. Polarizable force fields or three layer polarizable models further increase precision of the calculations,<sup>[61–63]</sup> similarly as for the fluctuating point charge model.<sup>[64]</sup> The explicit approach is usually based on geometries obtained by molecular dynamics (MD) simulations and many solute-solvent clusters ("snapshots") need to be averaged for realistic simulations.<sup>[36,65–67]</sup>

Even more technologically advanced approach to the condensed state modeling is *ab initio* molecular dynamics (AIMD), where electrons in the solute and in the solvent are treated at the same quantum-chemical level. The nuclei still follow Newtonian mechanics, and the forces are usually determined by DFT. Vibrational frequencies and IR and VCD

intensities are obtained via Fourier transform and autocorrelation functions. In this way, part of the anharmonic effects is obtained as well.<sup>[68]</sup> Interesting AIMD applications appeared for solute-solvent chirality transfer<sup>[69]</sup> or modeling VCD spectra of a flexible molecule, 2-butanol.<sup>[70]</sup> The AIMD technique can also be extended to Raman scattering and Raman optical activity simulations.<sup>[71,72]</sup>

### Vibrational Circular Dichroism Enhanced by Molecular Condensation

Occasionally, observed CD intensity (the *g*-factor) is much larger than expected from the simple estimations presented above. Then we talk about “enhanced” CD. From electronic CD studies of nucleic acids, such phenomenon is known from 1970s as  $\psi$ -CD (psi for “polymer and salt induced”). Under certain conditions, such as the presence of polymers or salts of multivalent metals, DNA molecules forms ordered aggregates and measured CD significantly increases, typically about 10-times.<sup>[73]</sup> Unlike CD, unpolarized absorption remains almost unchanged by the aggregation.

This phenomenon is not fully understood, and some scientists even attribute it to some unknown measurement artifacts. Nevertheless, it is generally accepted that at least some of the enhancement comes from a long-range order and coherent coupling of individual chromophores – bases in case of nucleic acids, or amide groups in peptides.<sup>[74–78]</sup> In any case, the enhancement of CD through long-range order seems to be a useful indicator of certain macromolecular chiral forms or aggregates.

For VCD, the “ $\psi$ -effect” was first observed in 2002, when DNA double strands further condensed in the presence of  $\text{Cr}^{3+}$  ions.<sup>[79]</sup> The authors observed approximately 4-fold increase of VCD intensity, and using atomic force microscopy they could relate it to formation of larger DNA/metal aggregates. Soon after, similar DNA condensation effect was observed for  $\text{Mn}^{2+}$  ions.<sup>[80]</sup>

Somewhat later, even bigger enhancement was observed in VCD spectra of protein fibrils.<sup>[81,82]</sup> This generated considerable interest in the scientific community, because these “misfolded” insoluble protein and peptide forms, often referred to as amyloid fibrils, accompany many animal or human diseases, such as preliminary neurodegeneration (Alzheimer, Parkinson, mad-cow, ...).<sup>[83–86,87–90]</sup> The fibrils are difficult to study by NMR or x-ray techniques, and in VCD the optical spectroscopy provides an interesting alternative. Model systems *in vitro* can be relatively easily prepared from various proteins and peptides, for example, by pH and temperature variation.<sup>[91–94]</sup> Typically, a longer time (hours, days) is needed for a completed fibril growth.

In 2007, enhanced VCD of insulin and hen egg-white lysozyme was associated with a twisted/helical structure of the fibrils.<sup>[81]</sup> Empirically, five VCD signature bands in the amide I ( $\text{C}=\text{O}$  stretching,  $\sim 1650\text{ cm}^{-1}$ ) and amide II ( $\text{CN}$  stretching,  $\sim 1530\text{ cm}^{-1}$ ) regions were ascribed to amyloid fibril aggregation, but VCD patterns of different signs and shapes were found

for various proteins and peptides.<sup>[95–99]</sup> Even for the same protein, a slight variation in fibril preparation may significantly affect their morphology<sup>[100]</sup> and VCD.<sup>[101–105]</sup>

For example, different polymorphic forms of hen egg-white lysozyme, apo- $\alpha$ -lactalbumin, TTR peptide and HET-s prion protein were formed at different pH.<sup>[98]</sup> Figure 1 illustrates how IR and VCD spectra of hen egg-white lysozyme fibrils grown at various pH levels correlate with SEM and fluid-cell AFM microscopy images for two fibril types. As usual, IR spectra of different fibrils are similar. They are dominated by a split amide I signal ( $1623/1663\text{ cm}^{-1}$ ), typical for the  $\beta$ -sheet. The intensity of the  $1663\text{ cm}^{-1}$  peak slightly increases with pH. The VCD spectra vary more. At pH 2.7 (red line), a strong negative band at  $1610\text{ cm}^{-1}$  appears, but fibrils grown at low pH (1.0 – blue, 1.5 – green) exhibit about opposite VCD signal. Needless to say, the “enhanced” dissymmetry factor  $g \sim 10^{-2}$  is much larger compared to the usual values ( $g \sim 10^{-5}$ ) for chiral molecules in solutions. At pH 2.3, an equilibrium between the two fibril forms provides much lower VCD intensity (black). This interpretation is consistent with the SEM and ATM images – fibrils grown at higher pH are narrow and exhibit a left-handed twist, while fibrils grown at lower pH are flatter and not twisted.

A model designed to explain some characteristics of protein fibrils was proposed by Measey and Schweitzer-Stenner.<sup>[106]</sup> It was based on helically propagated twisted three-dimensional lattice of amide I groups represented by oscillators/transition electric dipole moments, deviating by 20 degrees from the  $\text{C}=\text{O}$  bond in the amide plane. Simulated VCD spectra provided patterns that could be related to the experiment, however, without significant enhancement. Similar results were achieved by a more systematic study using the same simplified model, where, however, 10–100 $\times$  enhancements were observed for certain arrangements of the amide chromophores.<sup>[78]</sup> Never-

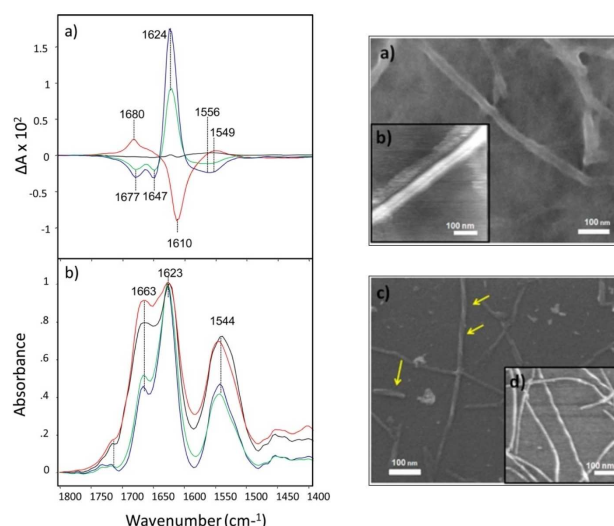


**Figure 1.** (Left) VCD (a) and IR (b) spectra of lysozyme fibrils grown at different pH (1.0 – blue, 1.5 – green, 2.3 – black and 2.7 – red) and (right) SEM (a, c) and fluid-cell AFM (b, d) images of fibrils grown at  $\text{pH} < 1.5$  (a, b) and  $\text{pH} > 2.7$  (c, d). Twisted parts are indicated by yellow arrows. Reproduced from ref. [98] with permission from the American Chemical Society.

theless, a credible theoretical basis for simulations of the experimental spectra is still missing.

### Vibrational Circular Dichroism of Crystals

In chiral crystals, which also attracted attention of the VCD technique, molecules are even more regularly ordered than in the fibrils. About 23% of all non-biological and 38% of all known crystals are chiral.<sup>[107]</sup> Enantiomerically pure chiral molecules always form chiral crystals.<sup>[108]</sup> But achiral molecules can also form them, if the crystal space group contains at least one screw axis other than 2<sub>1</sub>. Another possibility is a distortion/defect of ideal crystal structure, disrupting a long-range translational order and causing or contributing to the chirality.<sup>[109]</sup>

Kurouski et al. compared microcrystal VCD of a short peptide segment of human islet amyloid polypeptide (IAPP) with the spectra of fibrils formed from the same peptide. Both samples provided a significant enhancement, but the microcrystals gave a richer, more complex band structure.<sup>[110]</sup> Two polymorphic crystal forms of linezolid could be distinguished by VCD due to the differences in the carbonyl absorption spectral region.<sup>[111]</sup> Relatively weak VCD spectra were reported for several  $\alpha$ -<sup>[112]</sup> and cyclic  $\beta$ -amino acids,<sup>[113]</sup> and indazoles.<sup>[114]</sup>

AIMD simulations were conducted to understand VCD spectra of L-alanine crystals (Figure 2).<sup>[115]</sup> An interesting enhancement mechanism was identified, where molecular vibrations with small VCD intensity in a molecule contribute to the enhanced VCD signal due to a helical arrangement in the crystal layers.

### Vibrational Circular Dichroism Enhancement in Metal Complexes

Unusually large VCD is also often observed for transition metal complexes, containing  $\text{Co}^{2+}$ ,<sup>[116-118]</sup>  $\text{Co}^{3+}$ ,<sup>[119]</sup>  $\text{Ni}^{2+}$ ,<sup>[120,121]</sup> and other coordinating ions.<sup>[122,123]</sup> Clearly, this effect must be different than for the condensation-induced enhancement observed for

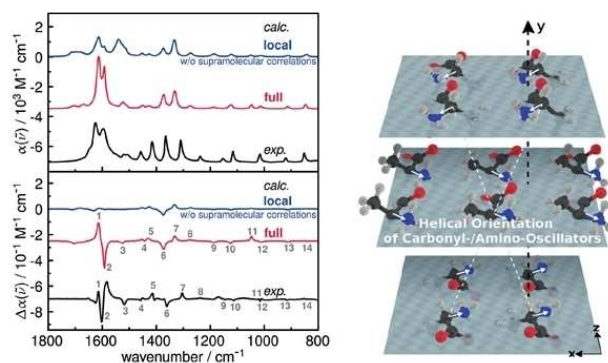


**Figure 2.** IR ( $\alpha$ ) and VCD ( $\Delta\alpha$ ) spectra of L-alanine crystals. Experimental spectra (black line) were measured in a form of nujol oil mull, calculated spectra (with local/full model) are in red/blue. On the right, the arrangement of alanine units in the crystal is plotted. Reproduced from ref. [115] with permission from Wiley-VCH.

the nucleic acids, fibrils and crystals. For some complexes, it has been explained by interaction of the vibrational transitions with low lying electronic states.<sup>[124]</sup> Therefore, its explanation goes beyond the Born-Oppenheimer approximation (In certain sense twice, because already the “ordinary” vibrational CD does).

The enhancement by coordination of  $\text{Co}^{2+}$  was explored for enantiomeric excess determination of several amino acids.<sup>[125]</sup> Enhanced monosignate and symmetry dependent VCD features have been observed for  $\text{Co}^{2+}$ /salicylaldiminato complexes.<sup>[126]</sup> Large VCD was reported for a tris(ethylenediaminato)(III)<sup>[127]</sup> and other  $\text{Co}^{3+}$  complexes.<sup>[128,129]</sup>

In some cases, however, the enhancement was explained by a charge transfer, that is within the Born-Oppenheimer theory.<sup>[127]</sup> In particular, the enhancement and shift of VCD N–H stretching vibrational bands in a  $\text{Co}^{3+}$  complex were attributed to the charge transfer from  $\text{Cl}^-$  ions to the N–H bond, symmetry of the vibrational modes, and changes of the electric and magnetic dipole transition moments. In Figure 3, experimental and calculated VCD spectra of the  $[\text{Co}(\text{en})_3]^{3+}$  complex are plotted. Both DFT functionals (OLYP, B3LYP) provide a reasonable but not perfect agreement with the experimental data. Similar analysis has been performed for VCD pattern in the fingerprint frequency region.<sup>[130]</sup>

### Vibrational Circular Dichroism Microsampling

Reduction of the sample size and mass is desirable for application in imaging of biological objects, studies of inhomogeneous samples, such as the fibrils, and for expensive compounds. Experimentally, this task is difficult because of the weakness of the signal and limitations of the infrared optics. Nevertheless, several studies appeared, such as that of Lu et al.<sup>[131]</sup> Using two additional fast-focusing lenses placed before and after the sample on a micro-XY positioning stage, they converted dual-PEM VCD instrument<sup>[132]</sup> into a microsampling device with a spatial resolution of about 1 mm, and used it to assess the heterogeneity of insulin and hen egg-white lysozyme amyloid fibril films.

An example of the spectra is plotted in Figure 4. The IR intensity at different spots reflects the thickness of the film, whereas the VCD differences suggest a very high chiral

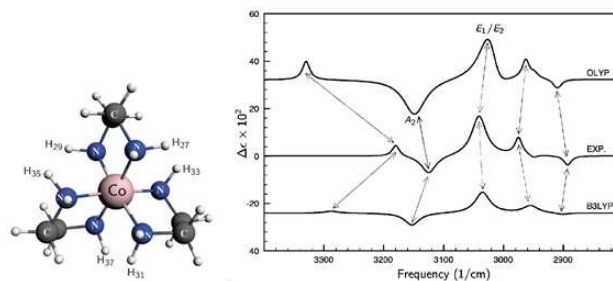


**Figure 3.** Experimental VCD spectrum of  $[\text{Co}(\text{en})_3]^{3+}$  in a 10-fold excess of chloride anion per complex (middle) and calculated spectra with two different DFT functionals, OLYP and B3LYP. Reproduced from refs. [127] and [130] with permission from the Royal Society of Chemistry.

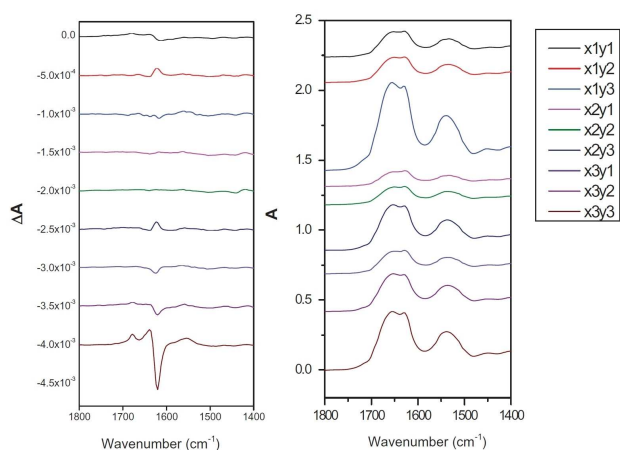


**Figure 4.** VCD (left) and IR (right) spectra of nine non-overlapping 1 mm big spots across a film of hen egg-white lysozyme amyloid fibrils. Reproduced from ref. [125] with permission from SAGE Publishing.

heterogeneity of the aggregates. In the future, this approach can perhaps be used in medical diagnostics, such as in objective evaluations of tissues in biopsies.

#### Vibrational Circular Dichroism of Ionic Liquids

Salts that are liquid at temperatures below 100 °C are called ionic liquids. They are useful in organic synthesis or “green” chemistry.<sup>[133,134]</sup> Chiral ionic liquids may be used for asymmetric synthesis<sup>[135–137]</sup> or analytical enantioseparations.<sup>[138,139]</sup> Although they are natural targets for chiroptical spectroscopies, so far they have been studied relatively rarely by these techniques.

Ouveley et al. used VCD and ROA to study alanine, valine or leucine, with 1-ethyl-3-methylimidazolium as a counterion (Figure 5).<sup>[140]</sup> Interestingly, VCD does not provide many characteristic features to distinguish the three compounds; more marker bands can be observed in the ROA spectrum. The 1-ethyl-3-methylimidazolium heavily contributes to the Raman and ROA spectra in 300–400 cm<sup>-1</sup> and 1300–1600 cm<sup>-1</sup>, that means that it also becomes chiral in the liquid. This interpretation of the spectra was supported by computational modeling.

#### Chiral Memory

Induction of chirality in achiral material and related phenomena attract attention both for applied chemistry and understanding of intermolecular interactions. Quite often, polymers are involved. An achiral polymer usually forms short helical segments. If it is doped with a small chiral molecule, the chirality can be propagated in a non-linear way and the whole system becomes optically active.<sup>[141,142]</sup> This was observed for poly(4-carboxyphenyl)doped with chiral amines,<sup>[143,144]</sup> poly(2,6-dimethyl-1,4-phenylene)doped with  $\alpha$ -pinene,<sup>[145]</sup> and other systems.<sup>[146–149]</sup> In many cases, the optical activity remains even

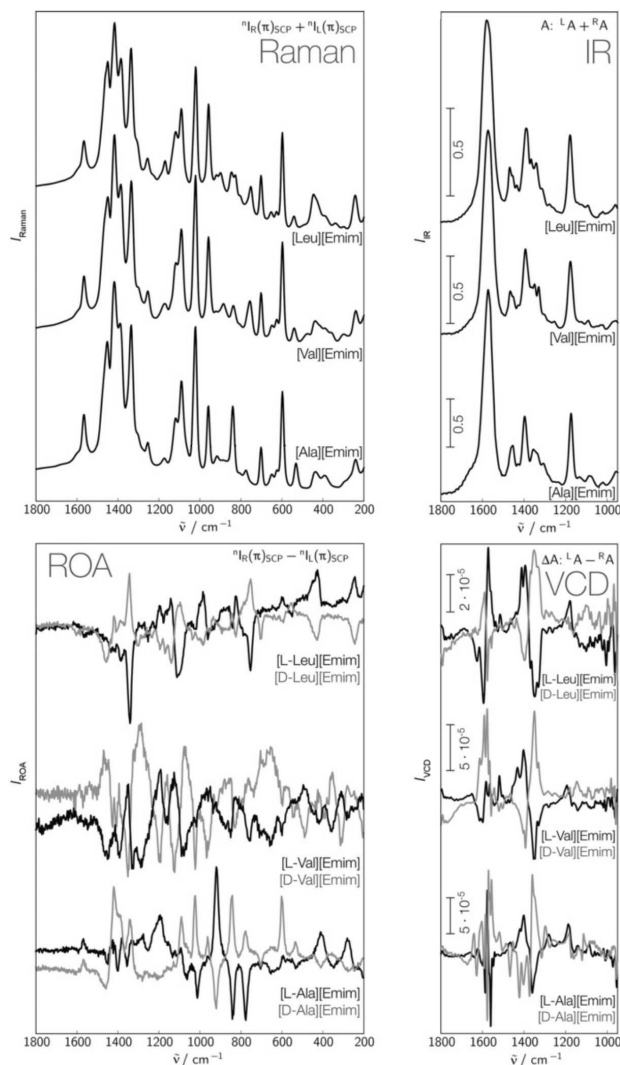


**Figure 5.** Raman, IR, ROA and VCD spectra of three ionic liquids, leucine, valine or alanine, with 1-ethyl-3-methylimidazolium counterion. Reproduced from ref. [140] with permission from Wiley-VCH.

after removal of the chiral dopant, i.e., the system “remembers” the chiral perturbation.<sup>[150–152]</sup>

As an example, syndiotactic polystyrene (s-PS) retains the induced chirality in temperatures up to 240 °C, which was attributed to chiral supramolecular structure, rather than to conformation of individual polymer chains.<sup>[153]</sup> Chiral s-PS films were also prepared with the presence of S and R carvone enantiomers.<sup>[154]</sup> As illustrated in Figure 6, both the host and guest molecules provide “mirror image” VCD spectra for opposite chirality, and the polymer optical activity remains almost unaltered when the chiral molecule is removed. The spectra suggest that molecular chirality of the guest molecule is overruled by the supramolecular chirality of the host polymer.

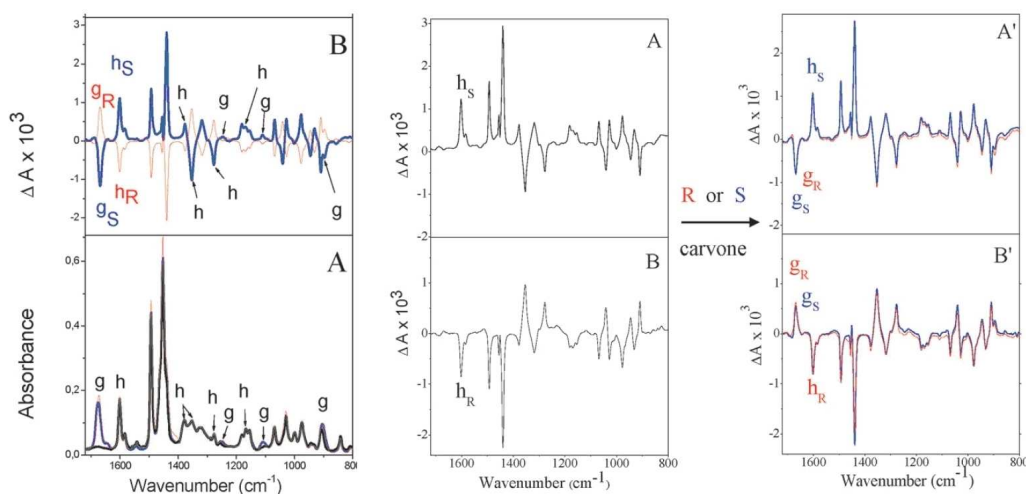


**Figure 6.** Example of chiral memory: (Left) IR (A) and VCD (B) spectra of the s-PS polymer film co-crystallized with S/R-carvone carvone, blue/red line, g and h letters mark bands of the guest and host molecules. VCD spectra (middle) after removal and (right) re-sorption of carvone. Reproduced from ref. [154] with permission from the Royal Society of Chemistry.

### Magnetic Vibrational Circular Dichroism

MVCD was firstly reported in 1981 for  $\text{CH}_3\text{I}$  and  $(\text{CH}_3)_4\text{Si}$ .<sup>[155]</sup> On a dedicated instrument,<sup>[156]</sup> other measurements of many small symmetric molecules followed soon, such as of methyl halides,<sup>[157]</sup>  $\text{CH}_3\text{OH}$  and  $\text{CH}_3\text{SH}$ .<sup>[158]</sup> Using the same “MVCD” instrument, low-lying electronic transitions could be measured as well, such as in organometallic compounds.<sup>[159]</sup> Later, “true vibrational” MVCD signals of porphyrins<sup>[160]</sup> and  $\text{C}_{60}$  fullerene<sup>[161]</sup> were obtained.

Interestingly, MVCD can also be measured for vibrational transitions in gases. On a good spectrometer rotational lines could be resolved and such spectra recorded, for example, for methane,<sup>[162,163]</sup> ammonia,<sup>[164]</sup> carbon monoxide,<sup>[165]</sup> hydrogen chloride,<sup>[166]</sup> and acetylene.<sup>[167]</sup>

At present, however, the MVCD technique does not seem to be pursued further. One reason is its high cost, in particular of liquid helium required to cool a superconductor magnet providing magnetic field up to  $\sim 10$  tesla. This is certainly a pity because for the gaseous spectra, for example, the theory can fully explain the experimental intensities and show that rotationally resolved MVCD reflects the Zeeman splitting of rotational energy levels and provides information on many molecular properties.<sup>[168,169]</sup> For example, for acetylene the vibrational magnetic dipole moment can be determined from MVCD,<sup>[170]</sup> and for NO, coupling of angular momenta can be studied.<sup>[171]</sup>

Condensed phase MVCD for a long time resisted through quantum chemical analysis, and available models explained it only qualitatively.<sup>[12,172,173]</sup> This changed in 2018 when MVCD intensities could be reproduced using common quantum-chemical software (Figure 7).<sup>[13]</sup> The MVCD theory, similarly as for (electronic) MCD is based on the transition electric dipole moments perturbed by the magnetic field.<sup>[174]</sup> When worked out for the vibrations, derivatives of the axial atomic tensor

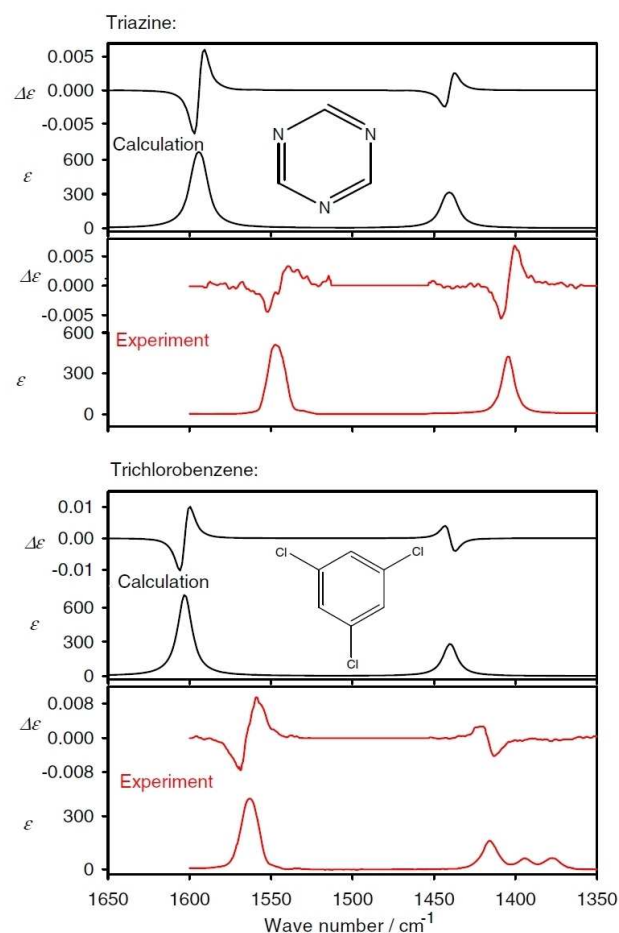


**Figure 7.** Triazine (top) and 1,3,5-trichlorobenzene (bottom), comparison of experimental and calculated (B3LYP/6-311 + +G\*\*) MVCD spectra. Reproduced from ref. [13] with permission from the American Physical Society.

with respect to nuclear coordinates appear crucial for the intensities.<sup>[13]</sup>

## Raman Optical Activity

### Raman Optical Activity of Saccharides

For sugars and related compounds ROA is often the most convenient technique. These molecules mostly lack a chromophore suitable for ECD, are investigated in solutions or do not provide crystals needed for x-ray crystallography, do not have distinct VCD bands, etc. In ROA, however, specific spectral features can usually be found, as shown, for example, for simple monosaccharides,<sup>[175,176]</sup> disaccharides,<sup>[177]</sup> polysaccharides,<sup>[178]</sup> cyclodextrins,<sup>[179]</sup> or heparin.<sup>[180]</sup> ROA bands, such as those around 430 and 917  $\text{cm}^{-1}$ , were also found to be very sensitive to the conformation.<sup>[179]</sup>

As usual in other cases, empirical analysis of the spectra may not be reliable.<sup>[181]</sup> For a long time quantum-mechanical spectral simulations have been complicated by saccharide flexibility and strong polar interactions with the solvent. Even for a simple sugar a large number of conformers including solvent molecules of the first solvation shell should be included. With improved computer hardware and programs, however, such computations quickly became a standard. A simplified energy weighting of pre-selected conformers was applied for a pyranose.<sup>[182]</sup> For gluconate, molecular dynamics and the Cartesian coordinate tensor transfer were used,<sup>[183]</sup> more elaborate methods of conformer sampling were applied later for methyl- $\beta$ -D-glucose<sup>[184]</sup> and similar monosaccharides.<sup>[185]</sup> Lately, an optimized computational protocol was proposed, balancing the accuracy and computational cost.<sup>[186]</sup>

ROA is also a promising technique to study the secondary and tertiary structure of polysaccharides.<sup>[180,187]</sup> So far, however, reliable computational methods are limited by molecular size, and spectral interpretations often revert to empirical rules and comparisons. These were used for the spectra of glycan and yeast external invertase<sup>[188]</sup> or chondroitin sulfate.<sup>[189]</sup> Composed glycoprotein molecules, such as mucin<sup>[190]</sup> or chondroitin,<sup>[189]</sup> remain a future challenge for the technique.

### Raman Optical Activity of Nucleic Acids

Compared to most saccharides or proteins, ROA of nucleic acids is more difficult to measure. The aromatic chromophores can decompose in the laser beam. As a rule, DNA is more stable than RNA. Also, the solubility is limited. Nevertheless, the first ROA spectra of single-stranded polynucleotides were reported already in 1997,<sup>[191]</sup> followed by other molecules<sup>[192]</sup> including double-stranded DNA.<sup>[193]</sup> The spectra provided insight into polynucleotide conformational dynamics.<sup>[194]</sup> Theoretical studies of the link between the spectra and the structure are rather rare so far.<sup>[195]</sup>

An interesting chapter in the spectroscopy was ROA measurement of whole viruses. Viral particles are to a large extent composed of nucleic acids, and viruses, such as filamentous bacteriophages, provided many well-resolved spectral features.<sup>[196–199]</sup> Fingerprint ROA patterns could be assigned to the GNRA tetraloop, pyrimidine-rich asymmetric bulge and a

base mismatch in ribosomal RNA of the encephalomyocarditis virus.<sup>[200,201]</sup> Unfortunately, no laboratory seems to continue the virus ROA research today.

### Protein Raman Optical Activity

Protein structure and dynamics are probably the most common targets of ROA spectroscopy, because of the biological implications, and relative simplicity of the ROA experiment.<sup>[202]</sup> The spectroscopy was employed to study protein folding,<sup>[203]</sup> dependence of the secondary structure on peptide chain length,<sup>[204]</sup> or the effect of protonation.<sup>[205]</sup> Blood plasma<sup>[206–208]</sup> and protein fibrils<sup>[209–211]</sup> were studied by ROA as well.

Early on, interpretation of the spectra was based on empirical rules.<sup>[212]</sup> Later, more universal density functional theory simulations provided insight, for example, into the ROA signal of the whole  $\beta$ -domain of the rat metallothionein protein.<sup>[213]</sup> For even bigger systems when the direct quantum-chemical approach may be inefficient or impossible, the Cartesian coordinate-based tensor transfer technique ("CCT") can be used, similarly as for VCD.<sup>[43]</sup> Atomic property tensors (force field, polarizability derivatives) are calculated for smaller chunks of the protein and transferred back on the original molecule. Usually, only very small error is introduced by this procedure if compared to a full quantum-chemical treatment.<sup>[42,43,214]</sup> This approach opens the combined ROA experimental/theoretical structural studies to sizable molecules, such as insulin<sup>[210]</sup> or even larger globular proteins (Figure 8).<sup>[215]</sup> A similar approach was introduced by Johannessen et al., based on oligopeptide fragment database.<sup>[216,217]</sup>

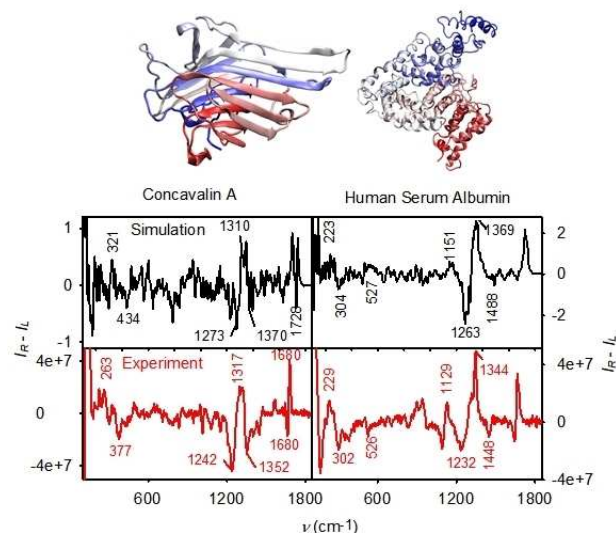


**Figure 8.** Example of ROA simulated and experimental spectra of a  $\beta$ -sheet (concanavalin A) and  $\alpha$ -helical (human serum albumin) protein. The 1230–1360  $\text{cm}^{-1}$  region seems to be the most indicative of the secondary structure. Reproduced from ref. [215] with permission from the American Chemical Society.

## Resonance Raman Optical Activity Techniques

To understand the concept of resonance, one has to realize the intensity expressions, such as those for backscattered polarized experiment,

$$\begin{aligned} \Delta I(\text{ROA}) &= I_R - I_L = 6K \sum_{\beta=1}^3 \sum_{\alpha=1}^3 (\alpha_{i,\alpha\alpha} \alpha_{i,\beta\beta} + 7\alpha_{i,\alpha\beta} \alpha_{i,\alpha\beta}) \\ I(\text{Ram}) &= I_R + I_L = \\ &48K \sum_{\beta=1}^3 \sum_{\alpha=1}^3 \left( 3\alpha_{i,\alpha\beta} G'_{i,\beta\alpha} - \alpha_{i,\alpha\alpha} G'_{i,\beta\beta} + \sum_{\varepsilon=1}^3 \sum_{\gamma=1}^3 \varepsilon_{\alpha\beta\gamma} \alpha_{i,\alpha\varepsilon} A_{i,\beta\gamma\varepsilon} \right), \end{aligned} \quad (11)$$

where  $\alpha$ ,  $G'$  and  $A$  are the electric, magnetic and quadrupole polarizability (derivatives with respect to a normal mode  $i$ ).<sup>[14]</sup> The electric dipole polarizability is

$$\alpha_{\alpha\beta} = \sum_{\varepsilon \neq n} \frac{2\omega_{jn}}{\hbar} \frac{\langle n | \mu_{\alpha} | j \rangle \langle j | \mu_{\beta} | n \rangle}{\omega_{jn}^2 - \omega^2}, \quad (12)$$

where  $n$  is molecular ground state,  $j$  is an excited state,  $\mu$  is the electric dipole moment,  $\hbar$  is the reduced Planck constant,  $\omega_{jn}$  is the transition frequency, and  $\omega$  is the excitation frequency. Similar expressions hold for  $G'$  and  $A$ . In the case that  $\omega$  is close to  $\omega_{jn}$ , the difference goes to zero and all polarizabilities, and consequently also Raman and ROA intensities, significantly grow.

As shown by Nafie,<sup>[218]</sup> in case of single electronic state resonance, also the *CID* may grow because the ROA intensity “borrows” the electronic transition momenta, usually bigger than the vibrational ones, and the ROA intensity becomes just proportional to the Raman signal,

$$\Delta I(\text{ROA}) = -\frac{g}{2} I(\text{RAM}) \quad (13)$$

where  $g$  is the dissymmetry factor of the electronic transition in resonance, say. Experimentally, this situation is easy to verify as we can obtain the  $g$ -factor from electronic CD signal measured at the laser excitation wavelength.<sup>[218]</sup> More complicated resonance Raman and ROA phenomena involving many electronic states are difficult to simulate. Time-dependent AIMD-based simulations seem to be extremely useful for these cases.<sup>[219,220]</sup>

In practice, the resonance can be both welcome because of the signal increase, and unwanted because it can destroy the sample or accompanying fluorescence can hide the desired Raman/ROA signal. The single state resonance was encountered in an europium complex,<sup>[221]</sup> carotenoid dyes,<sup>[222]</sup> two state resonance was reported for a copper complex,<sup>[223]</sup> etc.

For the most common 532 nm laser excitation the resonance occurs occasionally for color samples. For shorter UV wavelengths ( $\sim 200$  nm) the resonance condition  $\omega \sim \omega_{jn}$  is met for almost any molecule. Therefore “ultraviolet” ROA (UV ROA) is sometimes used as a synonym for resonance ROA, although practical realization of the experiment is rather different.

Additional signal enhancement for the excitation with UV light is achieved by increased scattering probability, proportional to  $\sim \lambda^{-4}$ . Encouraging results were reported for an UVROA instrument constructed in Glasgow.<sup>[224]</sup> In the future, exploration of even wider range of excitation frequencies for ROA is expected.

## Surface Enhanced Raman Optical Activity

Surface enhanced Raman scattering (SERS) is closely related to the resonance phenomenon. When close to metal (Cu, Ag, Au) surfaces, some molecules exhibit  $10^4$ – $10^{14}$  enhancement of the Raman scattering cross section; even “single-molecule experiments” were claimed.<sup>[225]</sup> Therefore, it seems natural to explore this phenomenon also for ROA.<sup>[226]</sup> However, this brings about many difficulties, such as polarization artifacts on the surface of the metal, destroying molecular ROA.<sup>[227–229]</sup> Another typical problem is the instability of colloidal particles, hampering accumulation of the spectra. Various ways were therefore suggested to stabilize the colloids, such as by a permanent coating or creating a protective polymer layer.<sup>[227,230]</sup>

Neither the theoretical approaches to model the SEROA and SERS phenomena are fully developed yet. Observed enhancements are assumed to be caused by a combination of large evanescent electromagnetic fields at the metal surface, enhancement by metal-molecule charge transfer and changes in the ground-state electronic structure of the molecule. Interesting results were obtained by simulation using clusters of observed molecules and metal atoms of the surface.<sup>[231–234]</sup>

In a phenomenological model, electromagnetic mutual polarization of a colloid and molecule was considered. The excitation laser light induces multipole moments in the investigated molecule, which then polarizes the metal particles (or metal surface extremities), and vice versa. The difficult perturbational expressions can be solved using the matrix polarization theory (MPT), which provides the total (effective) polarizations in a well tractable form. The MPT approach was applied to cysteine and ribose and provided realistic spectra.<sup>[235]</sup>

## Raman Optical Activity of Gases without and with Magnetic Field

Because the effect is so weak, ROA measurements are usually confined to the condensed phase. Nevertheless, in special cases, gaseous spectra were acquired as well, sometimes of surprising strength.

The first “ordinary” natural vibrational ROA spectrum was recorded for methyloxirane. The measurement was possible by a high vapor pressure of this molecule, resulting from its low boiling point (34 °C). Even then, artifact signal from the cell windows had to be very carefully subtracted, which was achieved by methyloxirane evaporation after the measurement, without moving the cell.<sup>[236]</sup> The experimental spectra were well reproduced by simulations including the rotational temperature-dependent line broadening. Having a molecule in vacuum is quite useful in tests of ab initio computational methods;

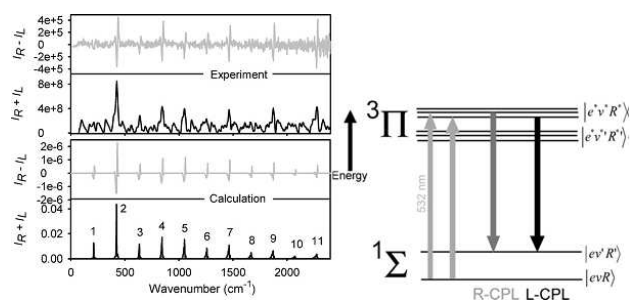


**Figure 9.** Experimental and simulated magnetic ROA ( $I_R - I_L$ ) and Raman ( $I_R + I_L$ ) spectra of iodine gas ( $I_2$ , peak numbers correspond to  $0 \rightarrow N$  vibrational transitions), and simplified scheme of the energy levels. The excited electronic states ( $e''$ ) are paramagnetic and significantly split in the magnetic field. Reproduced from ref. [15] with permission from Wiley-VCH.

indeed, the experiment was soon referred to in a work dealing with coupled cluster ROA simulations.<sup>[237]</sup>

Much stronger ROA signals were obtained from the gaseous paramagnetic  $NO_2$  molecule in a magnetic field of  $\sim 1.5$  tesla. Many phenomena contributed to the ROA intensity strength: the large molecular magnetic moment, Zeeman splitting of the rotational energy levels, strict selection rules of rotational/angular momentum wavefunctions, and a resonance of the 532 nm excitation light with many  $NO_2$  electronic transitions.<sup>[16]</sup> Further theoretical analysis showed that the paramagnetic ROA could be used to determine molecular polarizability components.

Even more unexpected was a similar observation for diamagnetic halogen gases ( $Cl_2$ ,  $Br_2$ , and  $I_2$ ). Based on the  $NO_2$  experience, their ROA signal should be negligible, because their magnetic moment is about 2000 times smaller. But one has to realize that their excited states are paramagnetic, and hence significantly split by the magnetic field as well. Raman spectroscopy, as a two-photon process, probes both the ground and excited state. Apart from the resonance, anharmonicity of the nuclear potential and relativistic spin-orbit interaction also contributed to the diamagnetic ROA of halogens, and simulations reproduced the experiment at least at a semi-quantitative level (Figure 9).<sup>[15]</sup> We also find the para and diamagnetic ROA experiments very useful to understand molecular behavior in more complicated situations, such as in resonance ROA of biologically relevant larger molecules in the condensed phase.

### Resonance Raman Optical Activity Chirality Transfer and "Ring of Fire"

Sometimes during a resonance ROA experiment ROA signal of the solvent can be observed, even when the solvent itself is not optically active. This "chirality transfer" from a chiral resonating molecule to the non-chiral environment was described for the "helquad" organic dye<sup>[238]</sup> as well as for some transition metal complexes.<sup>[239]</sup> For a nickel complex, the transfer was attributed to a "ring of fire", a space around the resonating complex and relatively far from it, where the solvent provides the biggest Raman and ROA signal. For simple solvents, the signs of ROA

bands could be even reproduced using a phenomenological transition polarizability model (Figure 10).<sup>[239]</sup> However, the model cannot explain the large CID ratios observed in the experiments.

### Aggregation-Induced Resonance Raman Optical Activity

Another example of the chirality transfer are carotenoid microcrystals/solutions, consisting mostly of achiral  $\beta$ -carotene, with a small amount of chiral  $\alpha$ -carotene and lutein.<sup>[240]</sup> The authors of such studies recognized that ROA of the sample was caused by a resonance of certain aggregated carotenoid complexes with the laser radiation and introduced the term aggregation-induced resonance Raman optical activity (AIRROA). In a typical experiment in solution, one-sign ROA pattern is obtained for the resonating carotenoid aggregates (for example, in an acetone/water mixture) and additional weak solvent (e.g., acetone) ROA bands appear due to the chirality transfer. The resonance can be conveniently monitored using UV absorption and ECD spectroscopy. This phenomenon is quite difficult to model computationally; nevertheless realistic aggregation and ECD spectral properties could be obtained by a combination of MD and DFT.<sup>[241]</sup>

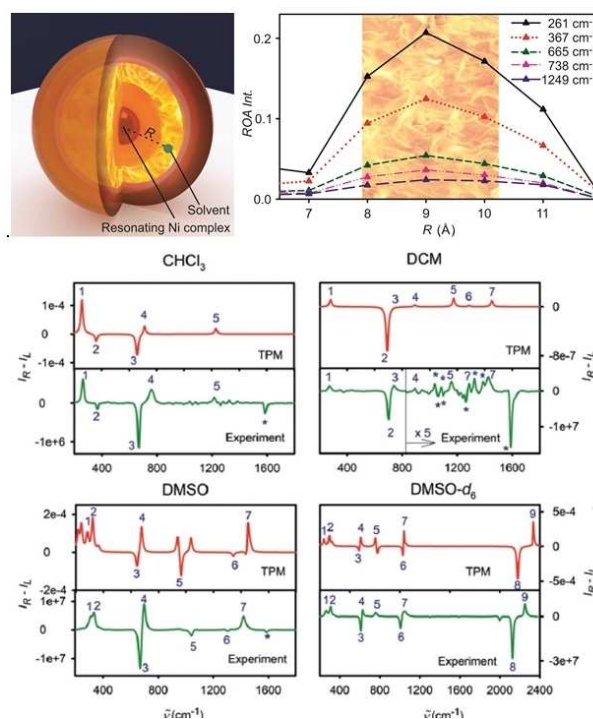


**Figure 10.** (Top) scheme of the "ring of fire" zone around the chiral complex acting in a resonance ROA chirality transfer to the solvent, and simulated intensity dependence of the ROA signal on the distance. (Bottom) examples of simulated and experimental spectra of four solvents. Reproduced from ref. [239] with permission from Wiley-VCH.

## Further Possibilities of ROA

All the examples mentioned above form only a tiny part of the world of chiral phenomena; others have been predicted theoretically<sup>[14,38]</sup> or may be expected in the future. One can consider different polarization schemes, excitation not only with visible and UV, but also red and near IR light,<sup>[242,243]</sup> or combination of ROA with circular polarized luminescence (CPL).<sup>[244]</sup> In particular, induced or magnetic CPL of lanthanides seem to be sensitively probing complex environment and well suitable for measurements with common ROA instruments.<sup>[245–252]</sup> Newest ROA spectrometers also measure as down as to  $\sim 50\text{ cm}^{-1}$  or up to  $4000\text{ cm}^{-1}$ , which brings new information about the molecules as well as new challenges to computational chemistry and theory.<sup>[253–255]</sup>

## Summary

We have briefly reviewed some results achieved in the field of vibrational optical activity in our and other laboratories, to illustrate the possibilities but also limits of the technique. We hope that the examples show the richness and future potential of the spectroscopic procedures. Chiroptical spectroscopy is a multi-disciplinary field touching chemistry, biology, medicine, mathematics, physics including light scattering theory and instrument manufacturing. As such, it is both intellectually challenging and useful, providing us with detailed insight into the world of chiral molecules.

## Acknowledgements

This work was supported by the Czech Science Foundation (18-05770S (P.B.), 20-10144S (J.K.)) and Ministry of Education (M.K., LTC17012/CA15214 and CZ.02.1.01/0.0/0.0/16\_019/0000729).

## Conflict of Interest

The authors declare no conflict of interest.

**Keywords:** chirality · circular dichroism · Raman optical activity · spectroscopy · vibrational spectra

- [1] M. Quack in *Molecular Parity Violation and Chirality: The Asymmetry of Life and the Symmetry Violations in Physics*, Vol. 26 (Eds.: K. Nishikawa, J. Maruani, E. J. Brändas, G. Delgado-Barrio, P. Piecuch), Springer Science, Dordrecht, 2012, pp.47–76.
- [2] N. A. McGuire, P. B. Carroll, R. A. Loomis, I. A. Finneran, P. R. Jewell, A. J. Remijan, G. A. Blake, *Science* 2016, 352, 1449–1452.
- [3] J. H. Christenson, J. W. Cronin, V. L. Fitch, R. Turlay, *Phys. Rev. Lett.* 1964, 13, 138–140.
- [4] L. Pasteur, *Ann. Chim. Phys.* 1848, 24, 442–459.
- [5] M. Mansuripur, *Optics Photonics News* 1999, 10, 32–36.
- [6] H. Rhee, Y. G. June, J. S. Lee, K. K. Lee, J. H. Ha, Z. H. Kim, S. J. Jeon, M. Cho, *Nature* 2009, 458, 310–313.
- [7] M. Oppermann, J. Spekowius, B. Bauer, R. Pfister, M. Chergui, J. Helbing, *J. Phys. Chem. Lett.* 2019, 10, 2700–2705.

- [8] G. Holzwarth, E. C. Hsu, H. S. Mosher, T. R. Faulkner, A. Moscovitz, *J. Am. Chem. Soc.* 1974, 96, 251–252.
- [9] L. A. Nafie, X. H. Qu, F. J. Long, T. B. Freedman, *Mikrochim. Acta* 1997, S14, 803–805.
- [10] L. D. Barron, M. P. Bogaard, A. D. Buckingham, *J. Am. Chem. Soc.* 1973, 95, 603–605.
- [11] W. Hug, G. Hangartner, *J. Raman Spectrosc.* 1999, 30, 841–852.
- [12] T. R. Devine, T. A. Keiderling, *J. Phys. Chem.* 1984, 88, 390–394.
- [13] T. A. Keiderling, P. Bouř, *Phys. Rev. Lett.* 2018, 121, 073201.
- [14] L. D. Barron, *Molecular Light Scattering and Optical Activity*, Cambridge University Press, Cambridge, UK, 2004.
- [15] J. Šebestík, J. Kapitán, O. Pačes, P. Bouř, *Angew. Chem. Int. Ed.* 2016, 55, 3504–3508; *Angew. Chem.* 2016, 128, 3565–3569.
- [16] J. Šebestík, P. Bouř, *Angew. Chem. Int. Ed.* 2014, 53, 9236–9239; *Angew. Chem.* 2014, 126, 9390–9393.
- [17] D. P. Craig, T. Thirunamachandran, *Molecular quantum electrodynamics*, Dover Publications, New York, 1998.
- [18] T. A. Keiderling in *Circular Dichroism*, Vol. (Eds.: N. Berova, K. Nakanishi, R. W. Woody), Wiley, New York, 2000, pp.621–666.
- [19] T. A. Keiderling in *Vibrational circular dichroism applications to conformational analysis of biomolecules*, Vol. (Ed. G. D. Fasman), Plenum, New York, 1996, pp.555–598.
- [20] W. R. Salzman, *J. Chem. Phys.* 1997, 107, 2175–2179.
- [21] P. J. Stephens, *J. Phys. Chem.* 1985, 89, 748–752.
- [22] R. D. Singh, T. A. Keiderling, *Biopolymers* 1981, 20, 237–240.
- [23] B. B. Lal, L. A. Nafie, *Biopolymers* 1982, 21, 2161–2183.
- [24] A. C. Sen, T. A. Keiderling, *Biopolymers* 1984, 23, 1519–1532.
- [25] A. C. Sen, T. A. Keiderling, *Biopolymers* 1984, 23, 1533–1545.
- [26] P. Pančoška, S. C. Yasui, T. A. Keiderling, *Biochemistry* 1989, 28, 5917–5923.
- [27] P. Pančoška, S. C. Yasui, T. A. Keiderling, *Biochemistry* 1991, 30, 5089–5103.
- [28] R. K. Dukor, T. A. Keiderling, *Biopolymers* 1991, 31, 1747–1761.
- [29] V. P. Gupta, T. A. Keiderling, *Biopolymers* 1992, 32, 239–248.
- [30] A. Annamalai, T. A. Keiderling, *J. Am. Chem. Soc.* 1987, 109, 3125–3132.
- [31] M. Gulotta, D. J. Goss, M. Diem, *Biopolymers* 1989, 28, 2047–2058.
- [32] W. Zhong, M. Gulotta, D. J. Goss, M. Diem, *Biochemistry* 1990, 29, 7485–7491.
- [33] L. Wang, T. A. Keiderling, *Biochemistry* 1992, 31, 10265–10271.
- [34] L. Yang, T. A. Keiderling, *Biopolymers* 1993, 33, 315–327.
- [35] L. J. Wang, L. G. Yang, T. A. Keiderling, *Biophys. J.* 1994, 67, 2460–2467.
- [36] V. Andrushchenko, D. Tsankov, M. Krasteva, H. Wieser, P. Bouř, *J. Am. Chem. Soc.* 2011, 133, 15055–15064.
- [37] J. R. Cheeseman, M. J. Frisch, F. J. Devlin, P. J. Stephens, *Chem. Phys. Lett.* 1996, 252, 211–220.
- [38] L. Nafie, *Vibrational optical activity: Principles and applications*, Wiley, Chichester, 2011.
- [39] G. Holzwarth, I. Chabay, *J. Chem. Phys.* 1972, 57, 1632–1635.
- [40] U. Narayanan, T. A. Keiderling, *J. Am. Chem. Soc.* 1983, 105, 6406–6410.
- [41] P. Bouř, J. Sopková, L. Bednářová, P. Maloň, T. A. Keiderling, *J. Comput. Chem.* 1997, 18, 646–659.
- [42] N. S. Bieler, M. P. Haag, C. R. Jacob, M. Reiher, *J. Chem. Theory Comput.* 2011, 7, 1867–1881.
- [43] S. Yamamoto, X. Li, K. Ruud, P. Bouř, *J. Chem. Theory Comput.* 2012, 8, 977–985.
- [44] R. A. G. D. Silva, J. Kubelka, S. M. Decatur, P. Bouř, T. A. Keiderling, *Proc. Natl. Acad. Sci. USA* 2000, 97, 8318–8323.
- [45] S. Yamamoto, M. Straka, H. Watarai, P. Bouř, *Phys. Chem. Chem. Phys.* 2010, 12, 11021–11032.
- [46] J. Kessler, V. Andrushchenko, J. Kapitán, P. Bouř, *Phys. Chem. Chem. Phys.* 2018, 20, 4926–4935.
- [47] V. Andrushchenko, P. Bouř, *J. Phys. Chem. A* 2007, 111, 9714–9723.
- [48] V. Andrushchenko, P. Bouř, *Chirality* 2010, 22, E96–E114.
- [49] K. V. J. Jose, D. Beckett, K. Raghavachari, *J. Chem. Theory Comput.* 2015, 11, 4238–4247.
- [50] K. V. J. Jose, K. Raghavachari, *Chirality* 2016, 28, 755–768.
- [51] B. Thapa, D. Beckett, K. V. J. Jose, K. Raghavachari, *J. Chem. Theory Comput.* 2018, 14, 1383–1394.
- [52] P. Wang, P. L. Polavarapu, *J. Phys. Chem. A* 2000, 104, 6189–6196.
- [53] J. R. Aviles-Moreno, E. U. Horno, F. P. Urena, J. J. L. Gonzalez, *Spectrochim. Acta Part A* 2011, 79, 767–776.
- [54] V. P. Nicu, E. J. Baerends, P. L. Polavarapu, *J. Phys. Chem. A* 2012, 116, 8366–8373.
- [55] M. Cossi, N. Rega, G. Scalmani, V. Barone, *J. Comput. Chem.* 2002, 24, 669–681.

- [56] J. Tomasi, B. Mennucci, R. Cammi, *Chem. Rev.* **2005**, *105*, 2999–3093.
- [57] M. L. Sanchez, M. A. Aguilar, F. J. Olivares del Valle, *J. Comput. Chem.* **1997**, *18*, 313–322.
- [58] A. Monari, J. L. Rivail, X. Assfeld, *Acc. Chem. Res.* **2013**, *46*, 596–603.
- [59] H. Gattuso, X. Assfeld, A. Monari in *Modeling DNA electronic circular dichroism by QM/MM methods and Frenkel Hamiltonian*, Vol. (Eds.: M. F. Ruiz-Lopez, F. J. Olivares del Valle), Springer Berlin Heidelberg, Berlin, Heidelberg, **2016**, pp.225–232.
- [60] J. Sjoqvist, M. Linares, K. V. Mikkelsen, P. Norman, *J. Phys. Chem. A* **2014**, *118*, 3419–3428.
- [61] T. A. Halgren, W. Damm, *Curr. Opin. Struct. Biol.* **2001**, *11*, 236–242.
- [62] C. Cappelli, *Int. J. Quantum Chem.* **2016**, *116*, 1532–1542.
- [63] T. Giovannini, M. Olszówka, C. Cappelli, *J. Chem. Theory Comput.* **2016**, *12*, 5483–5492.
- [64] S. W. Rick, B. J. Berne, *J. Am. Chem. Soc.* **1996**, *118*, 672–679.
- [65] V. Andrushchenko, L. Benda, O. Páv, M. Dračinský, P. Bouř, *J. Phys. Chem. B* **2015**, *119*, 10682–10692.
- [66] K. H. Hopmann, K. Ruud, M. Pecul, A. Kudelski, M. Dračinský, P. Bouř, *J. Phys. Chem. B* **2011**, *115*, 4128–4137.
- [67] I. Shahriar, M. K. Bin Islam, M. Iqfath, A. Rahman, M. A. Halim, *Theor. Chem. Acc.* **2019**, *138*, 32.
- [68] A. Scherrer, F. Agostini, D. Sebastiani, E. K. U. Gross, R. Vuilleumier, *J. Chem. Phys.* **2015**, *143*, 074106.
- [69] A. Scherrer, R. Vuilleumier, D. Sebastiani, *J. Chem. Phys.* **2016**, *145*, 084101.
- [70] M. Thomas, B. Kirchner, *J. Phys. Chem. Lett.* **2016**, *7*, 509–513.
- [71] S. Lubber, *J. Chem. Theory Comput.* **2017**, *13*, 1254–1262.
- [72] M. Brehm, M. Thomas, *J. Phys. Chem. Lett.* **2017**, *8*, 3409–3414.
- [73] L. S. Lerman, *Proc. Natl. Acad. Sci. USA* **1971**, *68*, 1886–1890.
- [74] M. H. Kim, L. Ulbarri, D. Keller, M. F. Maestre, C. Bustamante, *J. Chem. Phys.* **1986**, *84*, 2981–2989.
- [75] D. Keller, C. Bustamante, *J. Chem. Phys.* **1986**, *84*, 2972–2980.
- [76] D. Keller, C. Bustamante, *J. Chem. Phys.* **1986**, *84*, 2961–2971.
- [77] V. Andrushchenko, P. Bouř, *J. Comput. Chem.* **2008**, *29*, 2693–2703.
- [78] J. Průša, P. Bouř, *Chirality* **2018**, *30*, 55–64.
- [79] V. Andrushchenko, Z. Leonenko, D. Cramb, H. van de Sande, H. Wieser, *Biopolymers* **2002**, *61*, 243–260.
- [80] V. Andrushchenko, D. Tsankov, H. Wieser, *J. Mol. Struct.* **2003**, *661*, 541–560.
- [81] S. Ma, X. Cao, M. Mak, A. Sadik, C. Walkner, T. B. Freedman, I. K. Lednev, R. K. Dukor, L. A. Nafie, *J. Am. Chem. Soc.* **2007**, *129*, 12364–12365.
- [82] W. Dzwolak, *Chirality* **2014**, *26*, 580–587.
- [83] J. A. Hardy, G. A. Higgins, *Science* **1992**, *256*, 184–185.
- [84] C. M. Dobson, *Semin. Cell Dev. Biol.* **2004**, *15*, 3–16.
- [85] F. Chiti, C. M. Dobson, *Nat. Chem. Biol.* **2009**, *5*, 15–22.
- [86] A. Aguzzi, T. O'Connor, *Nat. Rev. Drug Discovery* **2010**, *9*, 237–248.
- [87] A. D. Wechalekar, J. D. Gillmore, P. N. Hawkins, *Lancet* **2016**, *387*, 2641–2654.
- [88] M. P. Mattson, *Nature* **2004**, *430*, 631–639.
- [89] [L. Breydo, J. W. Wu, V. N. Uversky, *Bba-Mol Basis Dis* **2012**, *1822*, 261–285.
- [90] P. M. Harrison, P. Bamborough, V. Daggett, S. B. Prusiner, F. E. Cohen, *Curr. Opin. Struct. Biol.* **1997**, *7*, 53–59.
- [91] M. Fandrich, M. A. Fletcher, C. M. Dobson, *Nature* **2001**, *410*, 165–166.
- [92] J. Goers, S. E. Permyakov, E. A. Permyakov, V. N. Uversky, A. L. Fink, *Biochemistry* **2002**, *41*, 12546–12551.
- [93] J. J. Lai, C. Zheng, D. H. Liang, Y. B. Huang, *Biomacromolecules* **2013**, *14*, 4515–4519.
- [94] L. Tjernberg, W. Hesia, N. Bark, J. Thyberg, J. Johansson, *J. Biol. Chem.* **2002**, *277*, 43243–43246.
- [95] V. Babenko, M. Piejko, S. Wójcik, P. Mak, W. Dzwolak, *Langmuir* **2013**, *29*, 5271–5278.
- [96] A. Fulara, A. Lakhani, S. Wójcik, H. Nieznańska, T. A. Keiderling, W. Dzwolak, *J. Phys. Chem. B* **2011**, *115*, 11010–11016.
- [97] D. Kurouski, K. Kar, R. Wetzal, R. K. Dukor, I. K. Lednev, L. A. Nafie, *FEBS Lett.* **2013**, *578*, 1638–1643.
- [98] D. Kurouski, X. F. Lu, L. Popova, W. Wan, M. Shanmugasundaram, G. Stubbs, R. K. Dukor, I. K. Lednev, L. A. Nafie, *J. Am. Chem. Soc.* **2014**, *136*, 2302–2312.
- [99] E. Van de Vondel, P. Baatsen, R. Van Elzen, A. M. Lambeir, T. A. Keiderling, W. A. Herrebout, C. Johannessen, *Biochemistry* **2018**, *57*, 5989–5995.
- [100] R. Kodali, R. Wetzal, *Curr. Opin. Struct. Biol.* **2007**, *17*, 48–57.
- [101] B. Nieto-Ortega, V. J. Nebot, J. F. Miravet, B. Escuder, J. T. L. Navarrete, J. Casado, F. J. Ramirez, *J. Phys. Chem. Lett.* **2012**, *3*, 2120–2124.
- [102] D. Kurouski, R. K. Dukor, X. Lu, L. A. Nafie, I. K. Lednev, *Chem. Commun.* **2012**, *48*, 2837–2839.
- [103] M. Krupová, J. Kapitán, P. Bouř, *ACS Omega* **2019**, *4*, 1265–1271.
- [104] M. Shanmugasundaram, D. Kurouski, W. Wan, G. Stubbs, R. K. Dukor, L. A. Nafie, I. K. Lednev, *J. Phys. Chem. B* **2015**, *119*, 8521–8525.
- [105] M. Pazderková, T. Pazderka, M. Shanmugasundaram, R. K. Dukor, I. K. Lednev, L. A. Nafie, *Chirality* **2017**, *29*, 469–475.
- [106] T. Measey, R. Schweitzer-Stenner, *J. Am. Chem. Soc.* **2011**, *133*, 1066–1076.
- [107] C. Dryzun, D. Avnir, *Chem. Commun.* **2012**, *48*, 5874–5876.
- [108] H. D. Flack, *Helv. Chim. Acta* **2003**, *86*, 905–921.
- [109] A. G. Shtukenberg, Y. O. Punin, A. Gujral, B. Kahr, *Angew. Chem. Int. Ed.* **2014**, *53*, 672–699; *Angew. Chem.* **2014**, *126*, 686–715.
- [110] D. Kurouski, J. D. Handen, R. K. Dukor, L. A. Nafie, I. K. Lednev, *Chem. Commun.* **2015**, *51*, 89–92.
- [111] J. Frelek, M. Gorecki, M. Laszcz, A. Suszczynska, E. Vass, W. J. Szczepek, *Chem. Commun.* **2012**, *48*, 5295–5297.
- [112] I. Kawamura, H. Sato, *Anal. Biochem.* **2019**, *580*, 14–20.
- [113] V. Declerck, A. Perez-Mellor, R. Guillot, D. J. Aitken, M. Mons, A. Zehacker, *Chirality* **2019**, *31*, 547–560.
- [114] J. J. L. González, F. P. Urena, J. R. A. Moreno, I. Mata, E. Molins, R. M. Claramunt, C. López, I. Alkorta, J. Elguero, *New J. Chem.* **2012**, *36*, 749–758.
- [115] S. Jähnigen, A. Scherrer, R. Vuilleumier, D. Sebastiani, *Angew. Chem. Int. Ed.* **2018**, *57*, 13344–13348.
- [116] R. Berardozi, E. Badetti, N. A. C. dos Santos, K. Wurst, G. Licini, G. Pescitelli, C. Zonta, L. Di Bari, *Chem. Commun.* **2016**, *52*, 8428–8431.
- [117] S. R. Domingos, A. Huerta-Viga, L. Baij, S. Amirjalayer, D. A. Dunnebie, A. J. Walters, M. Finger, L. A. Nafie, B. de Bruin, W. J. Buma, S. Woutersen, *J. Am. Chem. Soc.* **2014**, *136*, 3530–3535.
- [118] Y. He, X. Cao, L. A. Nafie, T. B. Freedman, *J. Am. Chem. Soc.* **2001**, *123*, 11320–11321.
- [119] C. Johannessen, P. W. Thulstrup, *Dalton Trans.* **2007**, 1028–1033.
- [120] C. J. Barnett, A. F. Drake, R. Kuroda, S. F. Mason, S. Savage, *Chem. Phys. Lett.* **1980**, *70*, 8–10.
- [121] M. C. K. Hiller, Y. Xu, *Phys. Chem. Chem. Phys.* **2012**, *14*, 12884–12891.
- [122] S. Lo Piano, S. Di Pietro, L. Di Bari, *Chem. Commun.* **2012**, *48*, 11996–11998.
- [123] H. Sato, T. Taniguchi, A. Nakahashi, K. Monde, A. Yamagishi, *Inorg. Chem.* **2007**, *46*, 6755–6766.
- [124] L. A. Nafie, *J. Phys. Chem. A* **2004**, *108*, 7222–7231.
- [125] L. Arrico, G. Angelici, L. Di Bari, *Org. Biomol. Chem.* **2017**, *15*, 9800–9803.
- [126] G. Pescitelli, S. Ludeke, M. Gorecki, L. Di Bari, *J. Phys. Chem. Lett.* **2019**, *10*, 650–654.
- [127] V. P. Nicu, J. Autschbach, E. J. Baerends, *Phys. Chem. Chem. Phys.* **2009**, *11*, 1526–1538.
- [128] T. B. Freedman, X. L. Cao, D. A. Young, L. A. Nafie, *J. Phys. Chem. A* **2002**, *106*, 3560–3565.
- [129] D. A. Young, T. B. Freedman, E. D. Lipp, L. A. Nafie, *J. Am. Chem. Soc.* **1986**, *108*, 7255–7263.
- [130] V. P. Nicu, M. Heshmat, E. J. Baerends, *Phys. Chem. Chem. Phys.* **2011**, *13*, 8811–8825.
- [131] X. F. Lu, H. G. Li, J. W. Nafie, T. Pazderka, M. Pazderková, R. K. Dukor, L. A. Nafie, *Appl. Spectrosc.* **2017**, *71*, 1117–1126.
- [132] L. A. Nafie, *Appl. Spectrosc.* **2000**, *54*, 1634–1645.
- [133] P. Wasserscheid, W. Keim, *Angew. Chem. Int. Ed.* **2000**, *39*, 3772–3789; *Angew. Chem.* **2000**, *112*, 3926–3945.
- [134] H. Weingaertner, *Angew. Chem. Int. Ed.* **2008**, *47*, 654–670; *Angew. Chem.* **2008**, *120*, 664–682.
- [135] Y. Jeong, Y. Park, J. S. Ryu, *Molecules* **2019**, *24*, 3349.
- [136] S. Z. Luo, X. L. Mi, L. Zhang, S. Liu, H. Xu, J. P. Cheng, *Angew. Chem. Int. Ed.* **2006**, *45*, 3093–3097; *Angew. Chem.* **2006**, *118*, 3165–3169.
- [137] M. Schmitkamp, D. Chen, W. Leitner, J. Klankermayer, G. Francio, *Chem. Commun.* **2007**, 4012–4014.
- [138] A. Hussain, M. F. AlAjmi, I. Hussain, I. Ali, *Crit. Rev. Anal. Chem.* **2019**, *49*, 289–305.
- [139] A. Singh, N. Kaur, H. K. Chopra, *Crit. Rev. Anal. Chem.* **2019**, *49*, 553–569.
- [140] P. Oulevey, S. Lubber, B. Varnholt, T. Burgi, *Angew. Chem. Int. Ed.* **2016**, *55*, 11787–11790; *Angew. Chem.* **2016**, *128*, 11962–11966.
- [141] E. Yashima, K. Maeda, *Macromolecules* **2008**, *41*, 3–12.
- [142] [P. Rizzo, G. Guerra, *Chirality* **2016**, *28*, 29–38.
- [143] E. Yashima, T. Matsushima, Y. Okamoto, *J. Am. Chem. Soc.* **1997**, *119*, 6345–6359.

- [144] E. Yashima, T. Matsushima, Y. Okamoto, *J. Am. Chem. Soc.* **1995**, *117*, 11596–11597.
- [145] O. Tarallo, V. Petraccone, C. Daniel, G. Fasano, P. Rizzo, G. Guerra, *J. Mater. Chem.* **2012**, *22*, 11672–11680.
- [146] E. Yashima, K. Maeda, T. Yamanaka, *J. Am. Chem. Soc.* **2000**, *122*, 7813–7814.
- [147] R. Sakai, T. Satoh, R. Kakuchi, H. Kaga, T. Kakuchi, *Macromolecules* **2003**, *36*, 3709–3713.
- [148] R. Sakai, T. Satoh, R. Kakuchi, H. Kaga, T. Kakuchi, *Macromolecules* **2004**, *37*, 3996–4003.
- [149] D. S. Schlitzer, B. M. Novak, *J. Am. Chem. Soc.* **1998**, *120*, 2196–2197.
- [150] E. Yashima, K. Maeda, Y. Okamoto, *Nature* **1999**, *399*, 449–451.
- [151] K. Maeda, K. Morino, Y. Okamoto, T. Sato, E. Yashima, *J. Am. Chem. Soc.* **2004**, *126*, 4329–4342.
- [152] H. Onouchi, D. Kashiwagi, K. Hayashi, K. Maeda, E. Yashima, *Macromolecules* **2004**, *37*, 5495–5503.
- [153] L. Guadagno, M. Raimondo, C. Silvestre, I. Immediata, P. Rizzo, G. Guerra, *J. Mater. Chem.* **2008**, *18*, 567–572.
- [154] P. Rizzo, E. Lepera, G. Guerra, *Chem. Commun.* **2014**, *50*, 8185–8188.
- [155] T. A. Keiderling, *J. Chem. Phys.* **1981**, *75*, 3639–3641.
- [156] T. A. Keiderling, *Appl. Spectrosc. Rev.* **1981**, *17*, 189–226.
- [157] T. R. Devine, T. A. Keiderling, *J. Chem. Phys.* **1983**, *79*, 5796–5801.
- [158] T. R. Devine, T. A. Keiderling, *Spectrochim. Acta Part A* **1987**, *43*, 627–629.
- [159] T. R. Devine, T. A. Keiderling, *J. Chem. Phys.* **1985**, *83*, 3749–3754.
- [160] P. V. Croatto, T. A. Keiderling, *Chem. Phys. Lett.* **1988**, *144*, 455–560.
- [161] C. N. Tam, B. Wang, T. A. Keiderling, W. G. Golden, *Chem. Phys. Lett.* **1992**, *198*, 123–127.
- [162] B. Wang, R. K. Yoo, P. V. Croatto, T. A. Keiderling, *Chem. Phys. Lett.* **1991**, *180*, 339–343.
- [163] B. L. Wang, T. A. Keiderling, *J. Phys. Chem.* **1994**, *98*, 3957–3963.
- [164] B. Wang, P. V. Croatto, R. K. Yoo, T. A. Keiderling, *J. Phys. Chem.* **1992**, *96*, 2422–2429.
- [165] B. Wang, T. A. Keiderling, *J. Chem. Phys.* **1993**, *98*, 903–911.
- [166] C. N. Tam, T. A. Keiderling, *J. Mol. Spectrosc.* **1993**, *157*, 391–401.
- [167] C. N. Tam, T. A. Keiderling, *Chem. Phys. Lett.* **1995**, *243*, 55–58.
- [168] P. Bouř, C. N. Tam, B. Wang, T. A. Keiderling, *Mol. Phys.* **1996**, *87*, 299–318.
- [169] C. N. Tam, P. Bouř, T. A. Keiderling, *J. Chem. Phys.* **1996**, *104*, 1813–1824.
- [170] P. Bouř, C. N. Tam, T. A. Keiderling, *J. Phys. Chem.* **1996**, *100*, 2062–2065.
- [171] B. Wang, P. Bouř, T. A. Keiderling, *Phys. Chem. Chem. Phys.* **2012**, *14*, 9586–9593.
- [172] L. Laux, V. Pultz, C. Marcott, J. Overend, A. Moscovitz, *J. Chem. Phys.* **1983**, *78*, 4096–4102.
- [173] M. Pawlikowski, T. A. Keiderling, *J. Chem. Phys.* **1984**, *81*, 4765–4773.
- [174] P. J. Stephens, *Annu. Rev. Phys. Chem.* **1974**, *25*, 201–232.
- [175] L. D. Barron, A. R. Gargaro, Z. Q. Wen, *Carbohydr. Res.* **1991**, *210*, 39–49.
- [176] E. W. Blanch, L. Hecht, L. D. Barron, *Protein Sci.* **1999**, *8*, 1362–1367.
- [177] A. F. Bell, L. Hecht, L. D. Barron, *J. Am. Chem. Soc.* **1994**, *116*, 5155–5161.
- [178] A. F. Bell, L. Hecht, L. D. Barron, *J. Raman Spectrosc.* **1995**, *26*, 1071–1074.
- [179] A. F. Bell, L. Hecht, L. D. Barron, *Chem. Eur. J.* **1997**, *3*, 1292–1298.
- [180] T. R. Rudd, R. Hussain, G. Siligardi, E. A. Yates, *Chem. Commun.* **2010**, *46*, 4124–4126.
- [181] F. Zhu, N. W. Isaacs, L. Hecht, L. D. Barron, *J. Am. Chem. Soc.* **2005**, *127*, 6142–6143.
- [182] S. Lubner, M. Reiher, *J. Phys. Chem. A* **2009**, *113*, 8268–8277.
- [183] J. Kaminsky, J. Kapitán, V. Baumruk, L. Bednářová, P. Bouř, *J. Phys. Chem. A* **2009**, *113*, 3594–3601.
- [184] J. R. Cheeseman, M. S. Shaik, P. L. A. Popelier, E. W. Blanch, *J. Am. Chem. Soc.* **2011**, *133*, 4991–4997.
- [185] A. Melcerová, J. Kessler, P. Bouř, J. Kaminsky, *Phys. Chem. Chem. Phys.* **2016**, *18*, 2130–2142.
- [186] V. Palivec, V. Kopecký, P. Jungwirth, P. Bouř, J. Kaminsky, H. Martinez-Seara, *Phys. Chem. Chem. Phys.* **2020**, *10.1039/c9cp05682c*.
- [187] N. R. Yaffe, A. Almond, E. W. Blanch, *J. Am. Chem. Soc.* **2010**, *132*, 10654–10655.
- [188] C. Johannessen, R. Pendrill, G. Widmalm, L. Hecht, L. D. Barron, *Angew. Chem. Int. Ed.* **2011**, *50*, 5349–5351; *Angew. Chem.* **2011**, *123*, 5461–5463.
- [189] V. Profant, C. Johannessen, E. W. Blanch, P. Bouř, V. Baumruk, *Phys. Chem. Chem. Phys.* **2019**, *21*, 7367–7377.
- [190] L. Ashton, P. D. A. Pudney, E. W. Blanch, G. E. Yakubov, *Adv. Colloid Interface Sci.* **2013**, *199–200*, 66–77.
- [191] A. F. Bell, L. Hecht, L. D. Barron, *J. Am. Chem. Soc.* **1997**, *119*, 6006–6013.
- [192] A. F. Bell, L. Hecht, L. D. Barron, *Biospectroscopy* **1998**, *4*, 107–111.
- [193] A. F. Bell, L. Hecht, L. D. Barron, *J. Am. Chem. Soc.* **1998**, *120*, 5820–5821.
- [194] A. F. Bell, L. Hecht, L. D. Barron, *J. Raman Spectrosc.* **1999**, *30*, 651–656.
- [195] K. J. Jalkanen, V. Würtz Jürgensen, A. Claussen, A. Rahim, G. M. Jensen, R. C. Wade, F. Nardi, C. Jung, I. M. Degtyarenko, R. M. Nieminen, F. Herrmann, M. Knapp-Mohammady, T. A. Niehaus, K. Frimand, S. Suhai, *Int. J. Quantum Chem.* **2006**, *106*, 1160–1198.
- [196] E. W. Blanch, A. F. Bell, L. Hecht, L. A. Day, L. D. Barron, *J. Mol. Biol.* **1999**, *290*, 1–7.
- [197] E. W. Blanch, D. J. Robinson, L. Hecht, L. D. Barron, *J. Gen. Virol.* **2001**, *82*, 1499–1502.
- [198] E. W. Blanch, D. J. Robinson, L. Hecht, C. D. Syme, K. Nielsen, L. D. Barron, *J. Gen. Virol.* **2002**, *83*, 241–246.
- [199] E. W. Blanch, L. Hecht, C. D. Syme, V. Volpetti, G. P. Lomonosoff, K. Nielsen, L. D. Barron, *J. Gen. Virol.* **2002**, *83*, 2593–2600.
- [200] A. J. Hobro, M. Rouhi, E. W. Blanch, G. L. Conn, *Nucleic Acids Res.* **2007**, *35*, 1169–1177.
- [201] A. J. Hobro, M. Rouhi, G. L. Conn, E. W. Blanch, *Vib. Spectrosc.* **2008**, *48*, 37–43.
- [202] L. D. Barron, L. Hecht, I. H. McColl, E. W. Blanch, *Mol. Phys.* **2004**, *102*, 731–744.
- [203] M. Kinalwa, E. W. Blanch, A. J. Doig, *Protein Sci.* **2011**, *20*, 1668.
- [204] V. Profant, V. Baumruk, X. Li, M. Šafařík, P. Bouř, *J. Phys. Chem. B* **2011**, *115*, 15079–11589.
- [205] A. Lorna, C. Johannessen, R. Goodacre, *Anal. Chem.* **2011**, *83*, 7978.
- [206] M. Tatarkovič, Z. Fišar, J. Raboch, R. Jiráč, V. Setnička, *Chirality* **2012**, *24*, 951–955.
- [207] L. Habartová, B. Bunganic, M. Tatarkovič, M. Zavoral, J. Vondroušová, K. Syslová, V. Setnička, *Chirality* **2018**, *30*, 581–591.
- [208] A. Snytnysya, M. Judexová, T. Hrubý, M. Tatarkovič, M. Miškovcová, L. Petruzelka, V. Setnička, *Anal. Bioanal. Chem.* **2013**, *405*, 5441–5453.
- [209] C. Mensch, A. Konijnenberg, R. Van Elzen, A. M. Lambeir, F. Sobott, C. Johannessen, *J. Raman Spectrosc.* **2017**, *48*, 910–918.
- [210] S. Yamamoto, J. Kaminsky, P. Bouř, *Anal. Chem.* **2012**, *84*, 2440–2451.
- [211] S. Yamamoto, H. Watarai, *Chirality* **2012**, *24*, 97–103.
- [212] Z. Q. Wen, L. Hecht, L. D. Barron, *Protein Sci.* **1994**, *3*, 435–439.
- [213] S. Lubner, M. Reiher, *J. Phys. Chem. B* **2010**, *114*, 1057–1063.
- [214] S. Yamamoto, P. Bouř, *Collect. Czech. Chem. Commun.* **2011**, *76*, 567–583.
- [215] J. Kessler, J. Kapitán, P. Bouř, *J. Phys. Chem. Lett.* **2015**, *6*, 3314–3319.
- [216] C. Mensch, L. D. Barron, C. Johannessen, *Phys. Chem. Chem. Phys.* **2016**, *18*, 31757–31768.
- [217] C. Mensch, C. Johannessen, *ChemPhysChem* **2018**, *19*, 3134–3143.
- [218] L. A. Nafie, *Chem. Phys.* **1996**, *205*, 309–322.
- [219] A. Baiardi, J. Bloino, V. Barone, *J. Chem. Theory Comput.* **2018**, *14*, 6370–6390.
- [220] J. Mattiat, S. Lubner, *J. Chem. Phys.* **2019**, *151*, 234110.
- [221] C. Merten, H. Li, X. Lu, A. Hartwig, L. A. Nafie, *J. Raman Spectrosc.* **2010**, *41*, 1563–1565.
- [222] G. Zajac, A. Kaczor, S. Buda, J. Młynarski, J. Frelek, J. Dobrowolski, M. Baranska, *J. Phys. Chem. B* **2015**, *119*, 12193–12201.
- [223] C. Merten, H. Li, L. A. Nafie, *J. Phys. Chem. A* **2012**, *116*, 7329–7336.
- [224] J. Kapitán, L. D. Barron, L. Hecht, *J. Raman Spectrosc.* **2015**, *46*, 392–399.
- [225] K. Kneipp, H. Kneipp, S. Abdali, R. W. Berg, H. Bohr, *Spectroscopy* **2004**, *18*, 433–440.
- [226] Z. Q. Wen, X. Cao, A. Vance, *J. Pharm. Sci.* **2008**, *97*, 2228–2241.
- [227] S. O. Pour, S. E. J. Bell, E. W. Blanch, *Chem. Commun.* **2011**, *47*, 4754–4756.
- [228] S. Abdali, *J. Raman Spectrosc.* **2006**, *37*, 1341–1345.
- [229] K. Osinska, M. Pecul, A. Kudelski, *Chem. Phys. Lett.* **2010**, *496*, 86–90.
- [230] S. O. Pour, L. Rocks, K. Faulds, D. Graham, V. Parchaňský, P. Bouř, E. W. Blanch, *Nat. Chem. Biol.* **2015**, *7*, 591–596.
- [231] L. Zhao, L. Jensen, G. C. Schatz, *J. Am. Chem. Soc.* **2006**, *128*, 2911–2919.
- [232] M. B. Jacobs, P. W. Jagodzinski, T. E. Jones, M. E. Eberhart, *J. Phys. Chem. C* **2011**, *49*, 24115–24122.
- [233] B. G. Janesko, G. E. Scuseria, *J. Chem. Phys.* **2006**, *125*, 124704.

- [234] S. L. Kleinman, E. Ringe, N. Valley, K. L. Wustholz, E. Phillips, K. A. Scheidt, G. C. Schatz, R. P. Van Duyne, *J. Am. Chem. Soc.* **2010**, *133*, 4115–4122.
- [235] V. Novák, J. Šebestík, P. Bouř, *J. Chem. Theory Comput.* **2012**, *8*, 1714–1720.
- [236] J. Šebestík, P. Bouř, *J. Phys. Chem. Lett.* **2011**, *2*, 498–502.
- [237] T. D. Crawford, K. Ruud, *ChemPhysChem* **2011**, *12*, 3442–3448.
- [238] J. Šebestík, F. Teplý, I. Císařová, J. Vávra, D. Koval, P. Bouř, *Chem. Commun.* **2016**, *52*, 6257–6260.
- [239] G. Li, J. Kessler, J. Cheramy, T. Wu, M. R. Poopari, P. Bouř, Y. Xu, *Angew. Chem. Int. Ed.* **2019**, *58*, 16495–16498.
- [240] [M. Dudek, E. Machalska, T. Oleszkiewicz, E. Grzebelus, R. Baranski, P. Szcześniak, J. Mlynarski, G. Zajac, A. Kaczor, M. Baranska, *Angew. Chem. Int. Ed.* **2019**, *58*, 8383–8388.
- [241] G. Zajac, E. Machalska, A. Kaczor, J. Kessler, P. Bouř, M. Baranska, *Phys. Chem. Chem. Phys.* **2018**, *20*, 18038–18046.
- [242] M. Unno, T. Kikukawa, M. Kumauchi, N. Kamo, *J. Phys. Chem. B* **2013**, *117*, 1321–1325.
- [243] T. Uchida, M. Unno, K. Ishimori, I. Morishima, *Biochemistry* **1997**, *36*, 324–332.
- [244] [G. Longhi, E. Castiglioni, J. Koshoubu, G. Mazzeo, S. Abbate, *Chirality* **2016**, *28*, 696–707.
- [245] T. Wu, J. Kapitán, V. Mašek, P. Bouř, *Angew. Chem. Int. Ed.* **2015**, *54*, 14933–14936.
- [246] T. Wu, P. Bouř, V. Andrushchenko, *Sci. Rep.* **2019**, *9*, 1068.
- [247] T. Wu, J. Kessler, J. Kaminský, P. Bouř, *Chem. Asian J.* **2018**, *13*, 3865–3870.
- [248] E. Brichtová, H. J. N. Vršková, J. Šebestík, P. Bouř, T. Wu, *Chem. Eur. J.* **2018**, *24*, 8664–8669.
- [249] T. Wu, P. Bouř, *Chem. Commun.* **2018**, *54*, 1790–1792.
- [250] T. Wu, J. Kapitán, V. Andrushchenko, P. Bouř, *Anal. Chem.* **2017**, *89*, 5043–5049.
- [251] T. Wu, J. Kessler, P. Bouř, *Phys. Chem. Chem. Phys.* **2016**, *18*, 23803–23811.
- [252] T. Wu, J. Průša, J. Kessler, M. Dračínský, J. Valenta, P. Bouř *Anal. Chem.* **2016**, *88*, 8878–8885.
- [253] J. Hudecová, V. Profant, P. Novotná, V. Baumruk, M. Urbanová, P. Bouř, *J. Chem. Theory Comput.* **2013**, *9*, 3096–3108.
- [254] P. Michal, R. Čelechovský, M. Dudka, J. Kapitán, M. Vůjtek, M. Berešová, J. Šebestík, K. Thangavel, P. Bouř, *J. Phys. Chem. B* **2019**, *123*, 2147–2156.
- [255] M. Hope, J. Šebestík, J. Kapitán, P. Bouř, *J. Phys. Chem. A* **2020**, *124*, 674–683.

---

Manuscript received: January 14, 2020  
 Revised manuscript received: February 18, 2020  
 Accepted manuscript online: February 19, 2020